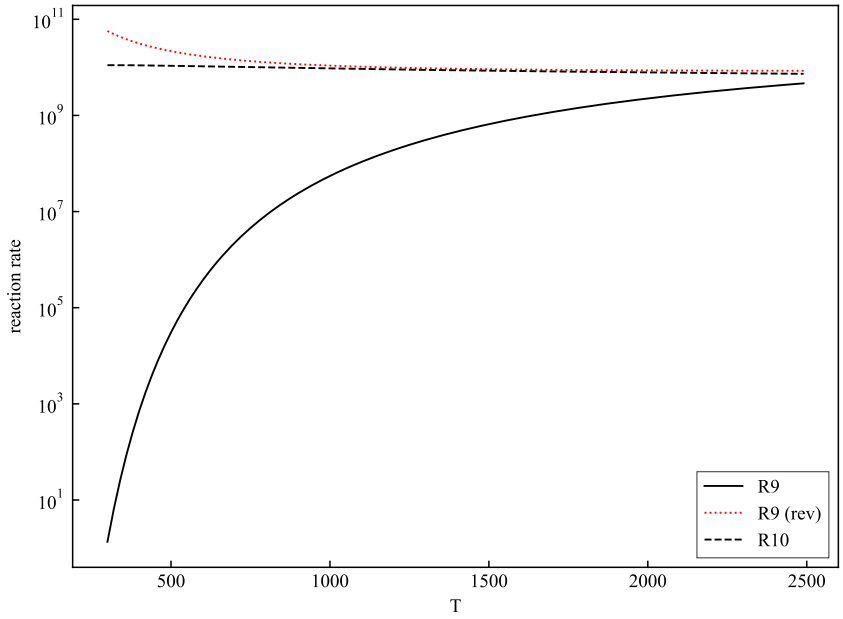

Figure 10.3: Forward and reverse rates for $H+O_2 \longrightarrow OH+O$ using the recommended values from Baulch et al. (2005) and the estimate k_f/K_c for the reverse rate.

low pressures, these reactions appear to depend explicitly on the pressure through the total concentration of the gas molecules. One-way of including this dependence is by introducing a third molecule into the reaction equation and to make the rate proportional to the concentration of that molecule. These processes are for this reason termed ter-molecular or three body reactions although they are really composite and consist of a sequence of bimolecular reactions.

Some important examples include the chain-termination reaction

$$H + O_2 + N_2 \longrightarrow HO_2 + N_2 \ , \tag{R14}$$

dissociation of diatomic molecules

$$N_2 + Ar \longrightarrow N + N + Ar \ , \tag{R15}$$

or the inverse process of recombination

$$N + N + Ar \longrightarrow N_2 + Ar \ . \tag{R16}$$

The third-body or chaperone molecule, N_2 or Ar in these examples, is often generically indicated as M although in many cases, the rate of reaction will depend significantly on the identity of M. This is often taken account of by assuming that each type of molecule has a collision efficiency α relative to some reference molecule, usually argon.

A three-body reaction will result in a change in the total number of molecules in addition to the release or absorption of thermal energy. In addition to chain termination, association reactions play a significant role in creating intermediate species and most importantly, in releasing energy through the recombination of intermediates to products. Two of the most important examples in combustion are:

$$H + OH + M \longrightarrow H_2O + M \quad \text{and} \tag{R17}$$

$$CO + O + M \longrightarrow CO_2 + M \ . \tag{R18}$$

Recombination or association can generically be written as

$$\mathrm{A} + \mathrm{B} + \mathrm{M} \longrightarrow \mathrm{AB} + \mathrm{M} \tag{R19}$$

and if this reaction is elementary, then the reverse reaction

$$\mathrm{AB} + \mathrm{M} \longrightarrow \mathrm{A} + \mathrm{B} + \mathrm{M} \tag{R20}$$

is equally plausible and the combination of forward and reverse reactions can be written

$$\mathrm{A} + \mathrm{B} + \mathrm{M} \rightleftarrows \mathrm{AB} + \mathrm{M} \tag{R21}$$

Using the formalism discussed in Section 10.2, the rate of progress can be written

$$\frac{1}{\nu_1}\frac{\mathrm{d}[\mathrm{M}_1]}{\mathrm{d}t} = \frac{1}{\nu_2}\frac{\mathrm{d}[\mathrm{M}_2]}{\mathrm{d}t} = \cdots = \frac{1}{\nu_K}\frac{\mathrm{d}[\mathrm{M}_K]}{\mathrm{d}t} = q = \left(\sum_{k=1}^{K}\alpha_k[\mathrm{M}_k]\right)\left(k_f\prod_{k=1}^{K}[\mathrm{M}_k]^{\nu'_k} - k_r\prod_{k=1}^{K}[\mathrm{M}_k]^{\nu''_k}\right) \tag{10.37}$$

The reaction rate constants k_f and k_r are usually given as functions of temperature using the modified Arrhenius format (10.10). As in the bi-molecular reaction case, for consistency only one of the two reaction rate constants are specified, usually the forward rate constant k_f and the reverse reaction rate constant can be computed using the equilibrium constant, $k_r = k_f/K_c$. The equilibrium constant for concentrations will depend on pressure because $\Delta\nu \neq 0$ for these cases. for example, for (R14), the equilibrium relation is

$$K_c = \left(\frac{[\mathrm{H}][\mathrm{O}_2]}{[\mathrm{HO}_2]}\right)_{eq}, \tag{10.38}$$

$$= \frac{1}{\mathcal{R}T}\left(\frac{P_\mathrm{H}P_{\mathrm{O}_2}}{P_{\mathrm{HO}_2}}\right)_{eq}, \tag{10.39}$$

$$= \frac{K_P(T)}{\mathcal{R}T} \tag{10.40}$$

Pressure-dependent or fall-off reactions

Ter-molecular reactions such as (R14) transition to uni-molecular reactions with increasing pressure.

$$\mathrm{H} + \mathrm{O}_2 \longrightarrow \mathrm{HO}_2 \tag{R22}$$

At low pressures, the forward reaction rate (R14) the value $k_o = 6.37{\times}10^{20}T^{-1.72}\exp -524.8/\mathcal{R}T$ and at high pressures, the forward reaction rate of (R22) is $k_\infty = 4.65{\times}10^{12}T^{0.44}$, see Baulch et al. (2005). The combined pressure dependent reaction, including the reverse process, is written as

$$\mathrm{H} + \mathrm{O}_2\ (+\mathrm{M}) \rightleftarrows \mathrm{HO}_2\ (+\mathrm{M}) \tag{R23}$$

and the effective forward reaction rate is described by a pressure-dependent rate constant $k_f(T,P)$. The simplest model (Gardiner, 1984, Laidler, 1987, Kee et al., 2003) is based on the notion that the reaction proceeds in two steps. First, the creation of an excited species through collisions of the reactants. For our example reaction, this is

$$\mathrm{H} + \mathrm{O}_2 \rightleftarrows \mathrm{HO}_2^* \quad , \qquad \text{forward rate:} \quad k_{f1}$$

Second, the stabilization of the excited species through collisions with the other molecules.

$$\mathrm{HO}_2^* + \mathrm{M} \rightleftarrows \mathrm{HO}_2 + \mathrm{M} \qquad \text{forward rate:} \quad k_{f2}$$

The excitation and de-excitation of the excited intermediate species HO_2^* are assumed to both occur sufficiently rapidly that the concentration of that species is in *quasi-steady state*.

$$\frac{\mathrm{d}[\mathrm{HO}_2^*]}{\mathrm{d}t} = 0 \tag{10.41}$$

Further approximating the concentration of HO_2 as negligible, the algebraic relationship between species obtained by the quasi-steady state approximation can be solved to compute the concentration of the excited intermediate state to be

$$[HO_2^*] = \frac{k_{1f}k_{2f}[H][O_2]}{k_{1r} + k_{2f}[M]} \, . \tag{10.42}$$

Substituting this into the reaction, the reaction progress can be computed to be

$$-\frac{d[H]}{dt} = -\frac{d[O_2]}{dt} = +\frac{d[HO_2]}{dt} = k_f[O_2][H] - k_r[HO_2] \tag{10.43}$$

where $k_r = k_f/K_c$ and K_c is the equilibrium constant for the association reaction

$$H + O_2 \rightleftarrows HO_2 \tag{10.44}$$

and k_f is the concentration-dependent forward reaction rate for the association reaction

$$k_f = \frac{k_{1f}k_{2f}[M]}{k_{1r} + k_{2f}[M]} \, . \tag{10.45}$$

This is equivalent to a pressure dependent reaction

$$k_f = k_\infty \frac{P_r}{1 + P_r} \tag{10.46}$$

using the ideal gas law to define $[M] = P/\mathcal{R}T$ and a reduced pressure

$$P_r = \frac{P}{P^*} \tag{10.47}$$

with a reaction reference pressure of

$$P^* = \frac{k_\infty \mathcal{R}T}{k_\circ} \tag{10.48}$$

The high pressure limit, $P_r \to \infty$, of the rate constant is

$$k_f \longrightarrow k_\infty = k_{1f} \tag{10.49}$$

and the reaction progress equation is

$$-\frac{d[H]}{dt} = -\frac{d[O_2]}{dt} = +\frac{d[HO_2]}{dt} = k_\infty[O_2][H] - \frac{k_\infty}{K_c}[HO_2] \, . \tag{10.50}$$

The low pressure limit, $P_r \to 0$, is

$$k_f \longrightarrow k_\circ[M] = \frac{k_{1f}k_{2f}}{k_{1r}}[M] \, . \tag{10.51}$$

and the reaction progress equation is

$$-\frac{d[H]}{dt} = -\frac{d[O_2]}{dt} = +\frac{d[HO_2]}{dt} = k_o[M][O_2][H] - \frac{k_o}{K_c}[M][HO_2] \, . \tag{10.52}$$

A refinement of the reaction rate pressure dependence (10.46) is to introduce an empirical correction factor $F(T, P_r)$ that can be used to better fit experimental data or reaction rate computations. A common model that is used in combustion reaction networks is the *Troe* function (Kee et al., 2003, Section 9.4); the parameters used by this function are supplied as part of the Cantera `.cti` reaction network data files. The reaction rate is modeled as

$$k_f = k_\infty \frac{P_r}{1+P_r} F(P_r, T) \; . \tag{10.53}$$

and the high and low pressure reaction rate constants k_∞ and k_o are functions of temperature using the modified Arrhenius format (10.10) with distinct parameters for each as determined by a combination of measurement (primarily for k_o) and computation or estimation (primarily for k_∞). The rate constants used in the Burke et al. (2012) reaction mechanism provided as part of the SDToolbox CTI resources use the Troe formulation for F.

The fall-off effect for reaction (R23) is shown in Fig. 10.4. The large decrease in reaction rate constants with decreasing or falling pressure is what give rises to the terminology *fall-off* effect. Three features standout and are common to all reactions of this type: first, the falloff effect is much more pronounced at low temperatures than high temperatures; second, the reverse reaction also has a fall-off effect; third, in order for the high-pressure limit to be reached, the pressure must be quite high (100 to 1000 atm) compared to typical gas-phase combustion conditions.

For consistency with the low-pressure limit of three-body reactions (R21) and the computation of reaction progress (10.37), the collision efficiency is included in computing the effective molar concentration of the third body [M] and the parameter P_r.

$$P_r = \frac{k_o}{k_\infty} \sum_{k=1}^{K} \alpha_k [M_k] = \frac{k_o}{k_\infty} \frac{P}{\mathcal{R}T} \sum_{k=1}^{K} \alpha_k [X_k]$$

where X_k is the mole fraction of species k. The effective value of the reference pressure is

$$P^* = \frac{k_\infty}{k_o} \frac{\mathcal{R}T}{\sum_{k=1}^{K} \alpha_k [X_k]}$$

For (R23), the reference pressure is $5.67{\times}10^7$ Pa at 600 K and $3.69{\times}10^9$ Pa at 2500 K. These pressures are quite high compared to conditions encountered in most combustion applications but may be relevant behind sufficiently strong shock waves in high-pressure situations like internal-combustion engines or some deflagration-to-detonation transition scenarios.

Another reaction that plays an important role in high-pressure and low-temperature combustion is the decomposition of hydrogen peroxide

$$H_2O_2 \; (+M) \rightleftarrows OH + OH \; (+M) \quad . \tag{R24}$$

The reaction progress equation based on the reaction rate k_f incorporating the fall-off factor is

$$-\frac{\mathrm{d}[H_2O_2]}{\mathrm{d}t} = +\frac{1}{2}\frac{\mathrm{d}[OH]}{\mathrm{d}t} = k_f[H_2O_2] - \frac{k_f}{K_c}[HO]^2 \; . \tag{10.54}$$

The reaction rates as a function of temperature and pressure are shown in Figure 10.5. The fall-off effect is qualitatively similar to (R23) and the magnitudes of the reference pressures: $3.11{\times}10^7$ Pa at 600 K and $1.25{\times}10^9$ pa at 2500 K are comparable.

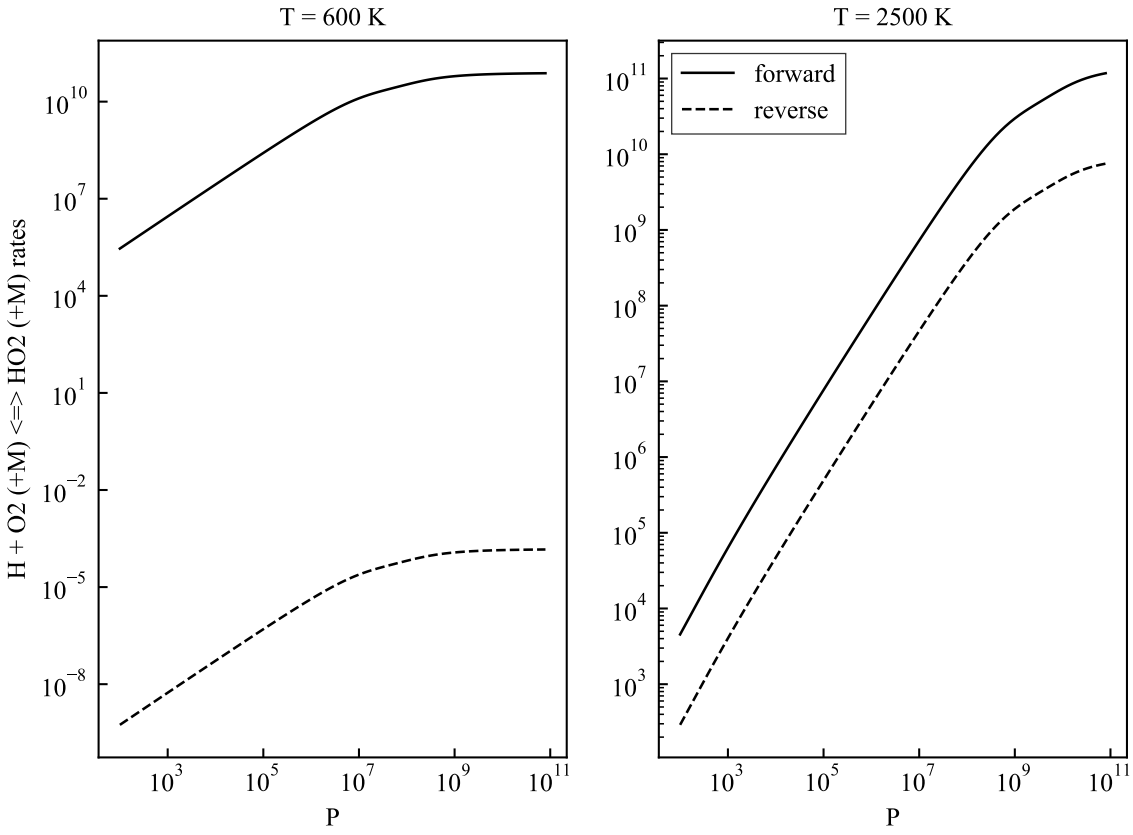

Figure 10.4: Evaluation of rate constants for (R23) as a function of pressure for two temperatures using the Burke et al. (2012) rate constant parameters and an atmosphere consisting of stoichiometric hydrogen-air combustion products in equilibrium at the specified temperatures and pressures.

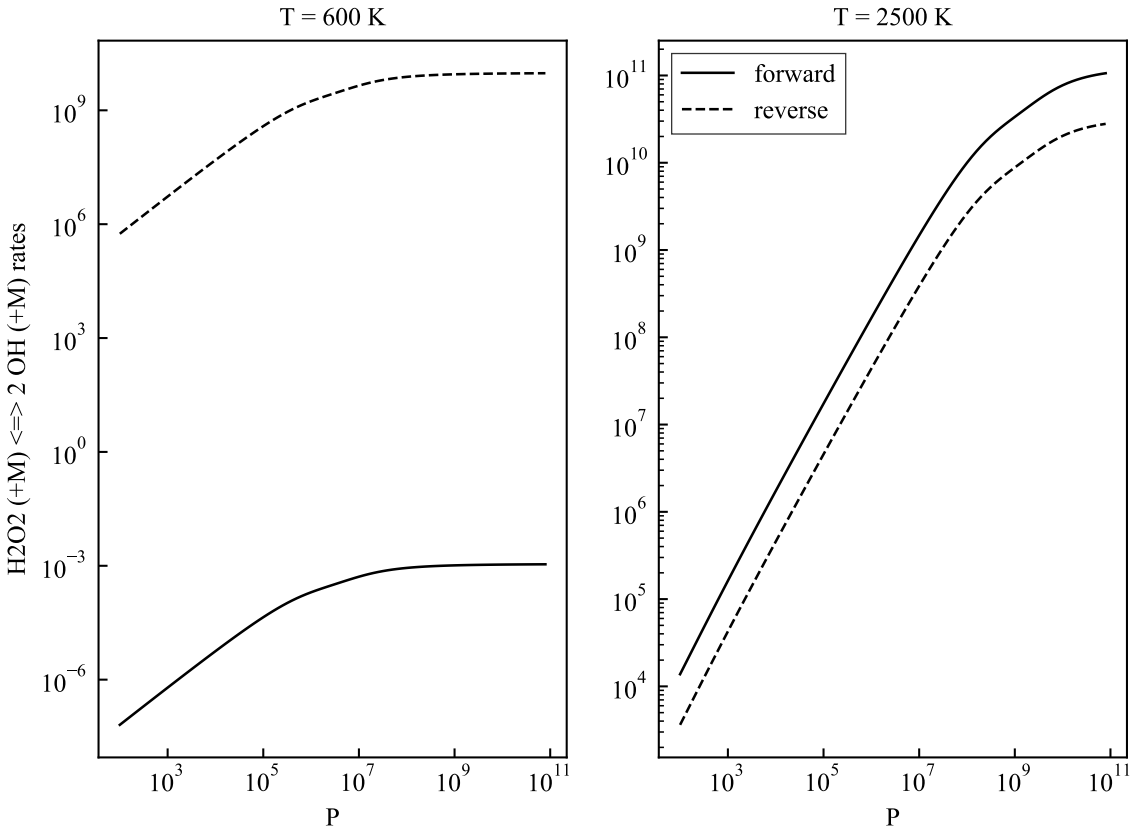

Figure 10.5: Evaluation of rate constants for (R24) as a function of pressure for two temperatures using the Burke et al. (2012) rate constant parameters and an atmosphere consisting of stoichiometric hydrogen-air combustion products in equilibrium at the specified temperatures and pressures.

10.4 Reaction Networks

Reaction mechanisms for even the simplest fuel-oxidizer systems like H_2-O_2 consist of a network of reactions that serve to transform the reactants into products through series and parallel reactions involving a numerous intermediate species. Each of these reactions $j = 1, 2, \ldots J$ has associated reaction rate constants $k_{f,j}$ and $k_{r,j}$, and stoichiometric coefficients ν''_{kj}, ν'_{kj} that define the rate of progress q_j for reaction j given the composition, pressure and temperature of the mixture. The net molar rate of production per unit volume of species k due to creation and destruction by all the reactions is

$$\dot{\omega}_k = \sum_{j=1}^{J} \nu_{kj} \dot{q}_j \qquad \nu_{kj} = \nu''_{kj} - \nu'_{kj} \tag{10.55}$$

The net rate of mass of species k generated per unit volume is $\mathcal{W}_k \dot{\omega}_k$. In a a reacting flow without diffusive transport, the mass balance equation for each species is (9.21)

$$\frac{\partial}{\partial t}(\rho Y_k) + \nabla \cdot (\rho \mathbf{u} Y_k) = \mathcal{W}_k \dot{\omega}_k \qquad (k = 1, \ldots, K) \,, \tag{10.56}$$

and further simplification leads to the most convenient expression for further use in formulating the reacting flow equations

$$\frac{\mathrm{D}Y_k}{\mathrm{D}t} = \frac{\mathcal{W}_k \dot{\omega}_k}{\rho} \qquad (k = 1, \ldots, K) \,. \tag{10.57}$$

The molar concentrations of each species are related to the mass fractions by

$$[\mathrm{X}_k] = \frac{Y_k \rho}{\mathcal{W}_k} \tag{10.58}$$

so that the material derivative of the molar concentration of species X_k can be expressed as

$$\frac{\mathrm{D}[\mathrm{X}_k]}{\mathrm{D}t} = \dot{\omega}_k + [\mathrm{X}_k] \frac{1}{\rho} \frac{\mathrm{D}\rho}{\mathrm{D}t} \,. \tag{10.59}$$

which provides the interpretation of $\dot{\omega}$ as the molar reaction rate at constant mass density.

A species can be created or destroyed by both forward and reverse reactions. To examine the role of individual reactions and the collective actions of the reaction network, the contributions to the rate of progress for a reaction are written as the difference between the contributions of forward and reverse reactions.

$$\dot{q}_j = \dot{q}_{f,j} - \dot{q}_{r,j} \,. \tag{10.60}$$

For a binary reaction, the rate of progress (10.33) can be used to define these two components

$$\dot{q}_{f,j} = k_f \prod_{k=1}^{K} [\mathrm{M}_k]^{\nu'_{kj}} \,, \qquad \dot{q}_{r,j} = k_r \prod_{k=1}^{K} [\mathrm{M}_k]^{\nu''_{kj}} \,, \tag{10.61}$$

and a similar expression can be derived from the rate of progress (10.37) for ter-molecular reactions. The net reaction rate of a species i is

$$\dot{\omega}_k = \sum_{j=1}^{J} (\nu''_{kj} - \nu'_{kj})(\dot{q}_{f,j} - \dot{q}_{r,j}) \,. \tag{10.62}$$

$$= \underbrace{\left(\sum_{j=1}^{J} \nu''_{kj} \dot{q}_{f,j} + \sum_{j=1}^{J} \nu'_{kj} \dot{q}_{r,j} \right)}_{\text{creation}} - \underbrace{\left(\sum_{j=1}^{J} \nu'_{kj} \dot{q}_{f,j} + \sum_{j=1}^{J} \nu''_{kj} \dot{q}_{r,j} \right)}_{\text{destruction}} \tag{10.63}$$

$$= \dot{C}_k - \dot{D}_k \tag{10.64}$$

The terms $\dot{C}$ and $\dot{D}$ are both positive. When these are large and nearly equal, the net rate of change of species k will be slow in comparison to that of species with much larger magnitudes of $\dot{\omega}_i$ and the species k is said to be in *quasi-steady-state*, $\dot{\omega}_k \approx 0$. This defines a set of algebraic relationships between the species concentrations in the relevant reactions. These relationships can be used to make analytic approximations which sometimes lead to simplifications in the reaction network representation.

The creation and destruction rates for a species can also be defined for a single reaction

$$\dot{C}_{kj} = \nu''_{kj}\dot{q}_{f,j} + \nu'_{kj}\dot{q}_{r,j} \ , \tag{10.65}$$

$$\dot{D}_{kj} = \nu'_{kj}\dot{q}_{f,j} + \nu''_{kj}\dot{q}_{r,j} \ . \tag{10.66}$$

10.5 Molecular Collisions and Reaction Rates

Collisions between pairs of individual molecules are the essential mechanism underlying the chemical (Houston, 2001, Laidler, 1987) and physical (Vincenti and Kruger, 1965, Boyd and Schwartzentruber, 2017) processes in high-temperature gas dynamics . The outcome of these collisions depends essentially on the speed with which molecules approach each other (relative speed or energy in the center of mass) and the distance of closest approach during the collision. In a high-temperature gas, the statistical distribution of individual molecular velocities and trajectories results in a corresponding statistical distribution of relative speeds and closest approach distances. The collective behavior of a gas is a consequence of averaging over these parameters to determine the average outcomes of the enormous numbers of collisions occurring per second in a volume of gas. The description of these collisions and the averaging process is the topic of gas kinetics research which started in the 19th century with Maxwell and Boltzmann.

Collisions conserve energy and momentum and at low energies or large distances, the identities of the molecules, but result in the transfer of energy, momentum and molecules from one region of a flow to another. Although this seems paradoxical, it is the essence of the process of diffusive transport and results from colliding molecules originating from different locations in the flow. If the flow has gradients in properties that are significant at the molecular level, as occurs in boundary or shear layers, flames and shock waves, then the colliding molecules will come from regions with significantly different mean properties and collisions effectively transport those mean properties across those gradients.

Collisions that take place with high relative speeds and close approach distances, will also result in transfer of internal energy (vibration and rotation) and in extreme cases, the transfer between or separation of atoms within the colliding molecules, i.e., chemical reactions. At the highest collision speeds, dissociation of molecules into atoms or separation into ions and electrons (ionization) can take place. The evaluation of energy exchange rates between molecules or chemical reaction rates requires not only averaging over the collision parameters but considering the dynamics of the atomic and electronic motion that control the bonding between the atoms and the electronic

Relative Motion of Molecules

The motion of the molecules of a gas in thermal equilibrium can be described statistically by the Maxwell-Boltzmann distribution of velocities (McQuarrie, 1976, Boyd and Schwartzentruber, 2017). For a molecule of mass m, each velocity component has a probability distribution function

$$\mathcal{P}(v_i) = \left(\frac{m}{2\pi k_B T}\right)^{1/2} \exp\left(-\frac{m v_i^2}{2k_B T}\right) \ , \quad i = x, y, z \, . \tag{10.67}$$

The molecular speed $v = |\mathbf{v}| = \sqrt{v_x^2 + v_y^2 + v_z^2}$ distribution is

$$\mathcal{P}(v) = \left(\frac{m}{2\pi k_B T}\right)^{3/2} \exp\left(-\frac{m v^2}{2k_B T}\right) 4\pi v^2 \tag{10.68}$$

The likelihood of chemical reaction or energy transder during a collision depends on the kinetic energy with which molecules A and B collide. This can be characterized by *relative speed* $v_r = |\mathbf{v}_A - \mathbf{v}_B|$ of approach to the collision event and the masses of the molecules. The probability distribution of the mean relative speeds of two molecules A and B is of the same form as the speed $v_A = |\mathbf{v}_A|$ for an individual molecule but using a reduced *reduced* molecular mass

$$m_r = \frac{m_A m_B}{m_A + m_B} \ . \tag{10.69}$$

The mean relative speed is

$$\langle v_r \rangle = \left(\frac{8 k_B T}{\pi m_r} \right)^{1/2} \tag{10.70}$$

where $\langle \cdot \rangle$ indicate the average over the equilibrium distribution of speeds. For nitrogen at room temperature, $v_r = 660$ m·s^{-1}.

Collision Cross Section Consider two molecules, A and B, approaching each other. If we consider the molecules as "hard spheres" of diameter $d_A$and d_B, they will only collide if centers of the molecules approach closer than a distance $d_{AB} = 1/2(d_A + d_B)$. This is equivalent to a collision taking place if the projected trajectory of molecule A passes through an area equal to πd_{AB}^2 centered on molecule B. For that reason, this area is known as the *collision cross-section* σ_{AB}. A more realistic model, discussed at the end of this section, is that the molecules are not hard spheres and the collision cross section is not a constant but depends on the relative velocity or energy of the two molecules. First, we will give the results for the hard sphere model. The effective hard sphere diameter of nitrogen molecules is about 0.36 nm and $\sigma = 4 \times 10^{-19}$ m^{-2} at room temperature.

Mean Free Path Consider a single molecule A in a gas of B molecules in thermal equilibrium. Each collision[2] of A with a B molecule will result in a change in velocity and direction of A and a compensating change in B in order to conserve energy and momentum. For ideal gases, the collisions are sufficiently rare and of such short duration, that after N collsions the path of A appears as a series of straight segments of variable length $\ell_1, \ell_2, \ldots, \ell_N$ and assuming the molecule moves with speed v_r on each of these flights. The average length of these flights, ℓ is known as the *mean free path*. If there are n_B molecules per unit volume, then our A molecule will encounter exactly N B molecules within the total volume V_N of the cylinders of radius d_{AB} surrounding each of the flight paths

$$N = n_B \underbrace{\left(\sum_{i=1}^{N} \ell_i \sigma_{AB} \right)}_{V_N} \ . \tag{10.71}$$

Defining the average flight distance as

$$\ell = \lim_{N \to \infty} \sum_{i=1}^{N} \ell_i \tag{10.72}$$

we obtain the average mean free path

$$\ell = \frac{1}{n_B \sigma_{AB}} \tag{10.73}$$

[2]For the purpose of this initial discussion we only consider non-reactive elastic collisions.

This expression is approximate as it does not account for the fact that the molecules have a distribution of velocities, may have unequal masses, and short flights are more likely than longer flights. A more accurate model requires considering the dynamics of the collisions and the Maxwell-Boltzmann velocity distributions for both molecules (Vincenti and Kruger, 1965). The exact result for a hard sphere model of a a gas composed of only one type of molecule is

$$\ell = \frac{1}{\sqrt{2} n \sigma} \tag{10.74}$$

This simple model is frequently used for gas mixtures with average values of σ and the total density n. For example, in air at sea level, $n = 2.55 \times 10^{25}$ molecules·m^{-3} and using the cross section for N_2, the mean free path is predicted to be ℓ =69 nm, within 4% of the more accurate mixture computation of 66 nm.

Collision Frequency Using the simple approach for mean free path, the average time between collisions can be estimated as

$$< t_c > = \frac{\ell}{\langle v_r \rangle} \tag{10.75}$$

In air at sea level, the average time between collisions is 0.148 ns, which is $> 10^2$ times longer than the duration $d/\langle v_r \rangle = 0.55$ ps of the average collision. The relatively long time (and distance) between collision provides the justification for the ideal gas assumptions of neglecting the molecular size and interactions except during the actual collisions. The average number of collisions of a single A molecule with the B molecules taking place per unit time is the *collision frequency* z and is equal to the reciprocal of the average time between collisions

$$z = \frac{1}{\langle t_c \rangle} = \frac{\langle v_r \rangle}{\ell} \, . \tag{10.76}$$

Substituting the simple expression for ℓ, we obtain

$$z = n_B \langle v_r \rangle \sigma_{AB} \, . \tag{10.77}$$

for the rate at which a *single* A molecule collides with B molecules per unit volume and unit time. The total number of collisions Z_{AB} between *all* A and B molecules per unit volume and time is obtained by multiplying the rate for a single molecule by the number of A molecules per unit volume

$$Z_{AB} = n_A n_B \langle v_r \rangle \sigma_{AB} \, . \tag{10.78}$$

If the molecules are identical then this expression over-counts the collision rate by a factor of two becuase each collision terminate two flights of a molecule A

$$Z_{AA} = \frac{1}{2} n_A^2 \langle v_r \rangle \sigma_{AB} \, . \tag{10.79}$$

For identical molecules, $m_r = m/2$ and $\langle v_r \rangle = \sqrt{2} \langle v \rangle$.

Gas Mixtures For a mixture of K species, the net rate at which molecule A collides with all other species i in the mixture requires summing over the collision rates with all the species

$$z = \sqrt{\frac{8 k_B T}{\pi}} \sum_{i=1}^{K} n_i \sigma_{Ai} \sqrt{\frac{1}{m_A} + \frac{1}{m_i}} \tag{10.80}$$

The mean free path of molecule A in the mixture is

$$\ell = \frac{1}{\sum_{i=1}^{K} n_i \sigma_{Ai} \sqrt{1 + \frac{m_A}{m_i}}} \tag{10.81}$$

For a binary mixture with $m_A = m_B$, we recover the result given previously.

Realistic Cross Sections A more realistic molecular collision model is that the collision cross-section is a function of the relative speed between the collision partners $\sigma(v_r)$. The cross-section for a non-reactive or elastic collision increases with decreasing relative velocity, for a Lennard-Jones potential, $\lim_{v_r \to 0} \sigma \sim v_r^{-2/5}$ due to the attractive portion of the potential and for high speed, $\lim_{v_r \to \infty} \sigma \sim v_r^{-2/11}$ due to the repulsive portion of the potential (Levine and Bernstein, 1987, p. 84).

Considering a gas in thermodynamic equilibrium and averaging over the distribution relative speed, the collision rate is

$$z = n_B \langle v_r \sigma_{AB} \rangle \ .$$

where in general we must include the dependence of σ_{AB} on v_r, the orientation, and impact parameters of the colliding molecules when carrying out the averaging process. The total number of collisions Z_{AB} between all A and B molecules per unit volume and time is obtained by multiplying the rate for a single molecule by the number of A molecules per unit volume

$$Z_{AB} = n_A n_B \langle v_r \sigma_{AB} \rangle \ .$$

We can express with in terms of an effective average collision cross-section $\sigma(T)$ that is temperature dependent. The usual way in which this is taken into account for elastic collisions is through a nondimensional collision function Ω^* which is a function of the molecular potential parameters such as the Lennard-Jones potential.

$$\langle v \sigma_{AB} \rangle = \langle v_r \rangle \pi d_{AB}^2 \Omega^* \left(\frac{k_B T}{\epsilon_{AB}} \right) \ , \tag{10.82}$$

where $d_{AB} = 1/2(\varrho_A + \varrho_B)$ where ϱ_A and ϱ_B are the potential zero location. ϵ_A and ϵ_B are the potential well depths and $\epsilon_{AB} = \sqrt{\epsilon_A \epsilon_B}$. Curve fits to the collision function are given in Neufeld et al. (1972), $\Omega^{(1,1)*}$ is the appropriate choice for computing collision frequency. At high reduced temperatures, $T^* = k_B T/\epsilon \gg 1$, the reduced collision integral can be approximated as a constant, $\Omega^{(1,1)*} \to 0.5$, as shown in Fig. 10.6. The final result for the elastic collision rate in terms of the collision integral is

$$Z_{AB} = n_a n_b \langle v_r \rangle \pi d_{AB}^2 \Omega^* \ . \tag{10.83}$$

This result provides an upper bound on the rate of reaction or energy exchange in a gas (Chen et al., 2017). This also motivates the further development of reaction rate models through more sophisticated treatments of the cross section.

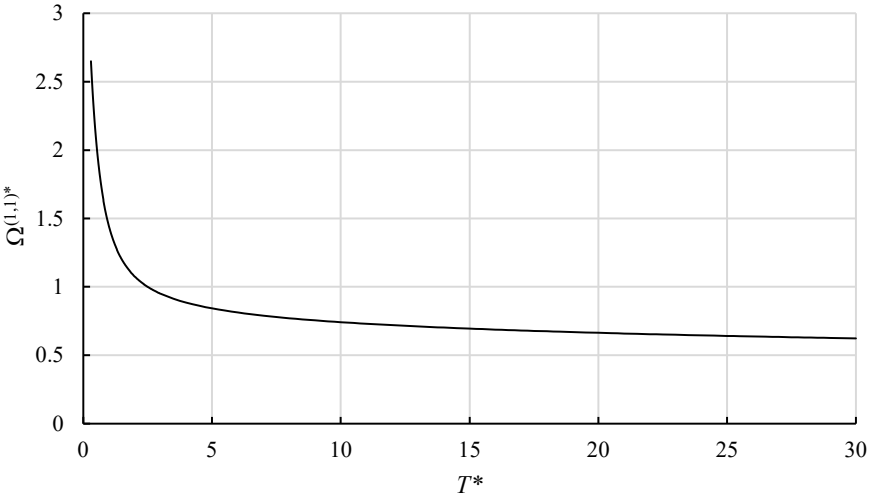

Figure 10.6: Reduced collision integral as a function of reduced temperature for Lennard-Jones potential .

Reaction Rates

Consider a bimolecular collision between species A and B

$$\text{A} + \text{B} \longrightarrow \text{Products} \tag{R25}$$

The number of reactive collisions of A and B molecules per unit volumes and time is the product of the collision rate Z_{AB} and the probability $\mathcal{P}_{AB}$ of reaction per collision. The rate of reaction of species A and B are

$$-\frac{\mathrm{d}n_A}{\mathrm{d}t} = -\frac{\mathrm{d}n_B}{\mathrm{d}t} \,, \tag{10.84}$$

$$= Z_{AB}\mathcal{P}_{AB} \,, \tag{10.85}$$

$$= \left(\frac{8k_BT}{\pi m_r}\right)^{1/2} \pi d_{AB}^2 \Omega^*(T) \mathcal{P}_{AB} n_A n_B \,. \tag{10.86}$$

In terms of the molar concentrations that are usually employed in chemical kinetics computations, this can be written

$$-\frac{\mathrm{d}[A]}{\mathrm{d}t} = -\frac{\mathrm{d}[B]}{\mathrm{d}t} = \left(\frac{8k_BT}{\pi m_r}\right)^{1/2} \pi d_{AB}^2 \Omega^* N_A \mathcal{P}_{AB} [A][B] \tag{10.87}$$

Comparing this with the usual bi-molecular rate expression

$$-\frac{\mathrm{d}[A]}{\mathrm{d}t} = -\frac{\mathrm{d}[B]}{\mathrm{d}t} = k(T)[A][B] \,, \tag{10.88}$$

we observe that the rate constant can be expressed as

$$k = \left(\frac{8k_BT}{\pi m_r}\right)^{1/2} \pi d_{AB}^2 \Omega^*(T) N_A \mathcal{P}_{AB} \,. \tag{10.89}$$

The largest value for $\mathcal{P}_{AB} = 1$, which means every pair of A-B collisions is reactive. This is the *collision limit* for the reaction rate and sets an upper bound on the rate constant $k \leq k_{col}$ where

$$k_{col} = \left(\frac{8k_BT}{\pi m_r}\right)^{1/2} \pi d_{AB}^2 \Omega^*(T) N_A \,. \tag{10.90}$$

See the discussion in Chen et al. (2017) for examples of how this can be used to check the values of rate constants for physical reasonableness. Elementary gas-phase bimolecular reactions can only occur if a collision occurs. When reaction rates are modeled with empirical expressions using parameters determined by optimizing the mechanism against sets of experimental data for properties like flame speed, shock tube or rapid compression machine induction times, the resulting rate constants may exceed the collision limit in some temperature ranges because the constraint $k(T) \leq k_{col}(T)$ is not enforced during optimization or checked when reaction rates are estimated with empirical methods. This can lead to unphysical results.

Activation Energy For exothermic reactions with a high probability of reaction taking place during a collision, the rate constant can be approximated using the collision-limit value of k discussed above. However, many reactions only take place with the relative collision velocities or equivalently, energy, exceed a critical or *activation* value. The empirical observation is that the reaction rate constant has the form pioneered by Arrhenius:

$$k = A \exp\left(-\frac{E_A}{\mathcal{R}T}\right) \tag{10.91}$$

using the standard chemical kinetics notation of a pre-exponential factor A and activation energy E_A (in molar units). In general, the pre-exponential factor is also a function of temperature which is modeled in the modified Arrhenius form prevalent in many chemical kinetics reaction rate mechanisms by including an additional term

$$k = AT^{\beta} \exp\left(-\frac{E_A}{\mathcal{R}T}\right) \tag{10.92}$$

where β is an empirical constant. A simple approach to modeling the effect of an activation energy at the molecular level is to incorporate a threshold energy ε_A in the cross section.

$$\sigma = 0 \text{ for } \varepsilon < \varepsilon_A \,, \text{ and } \sigma > 0 \text{ for } \varepsilon \geq \varepsilon_A \,. \tag{10.93}$$

A standard functional relationship that reproduces empirical Arrhenius dependence on temperature and approaches the collision limit at high energies is the *line of centers model* (Houston, 2001, Laidler, 1987)

$$\sigma = \begin{cases} 0 & \varepsilon < \varepsilon_A \\ \pi d^2 \left(1 - \dfrac{\varepsilon_A}{\varepsilon}\right) & \varepsilon \geq \varepsilon_A \end{cases} \tag{10.94}$$

Using the distribution function for relative velocity and averaging, the resulting reaction rate constant in molar units is

$$k = N_a \pi d_{AB}^2 \sqrt{\frac{8k_B T}{\pi m_r}} \exp\left(-\frac{E_a}{\mathcal{R}T}\right) \,, \tag{10.95}$$

where $E_a = N_a \varepsilon_A$. To go further in modeling reaction rates requires considering the electonic structure of the molecules, the resulting potential energy surfaces describing the interactions, the theory of the activated complexes formed during collision, and the statistical treatment of the atomic and molecular motions during the collision process, see the introductory discussions in Levine and Bernstein (1987), Houston (2001), Laidler (1987).

10.6 One-step Reactions

An empirical approach to treating reaction rates is to treat the reaction as occur through a single progress variable. This is known as a one-step or global reaction model (Westbrook and Dryer, 1981) and although not a reliable approach for quantitative prediction, has been widely used in numerical and analytical studies of the interaction of fluid dynamics and chemical reaction.

The basic notion is that the reaction between fuel $\mathcal{F}$ and oxidizer $\mathcal{O}$ or decomposition of a molecular explosive, form products $\mathcal{P}$. Schematically this can be represented for fuel-oxidizer mixtures as a global reaction

$$n_f \mathcal{F} + n_o \mathcal{O} \rightarrow n_p \mathcal{P} \tag{R26}$$

with a single rate of progress variable and reaction rate. In conventional terms, the rate of generation of products is expressed as

$$\frac{\mathrm{d}[\mathcal{P}]}{\mathrm{d}t} = \dot{\omega}_{\mathcal{P}} \,, \tag{10.96}$$

where the molar production rate is based on an empirical correlation motivated by the modified Arrhenius model of elementary reaction rates

$$\dot{\omega}_{\mathcal{P}} = [\mathcal{F}]^a [\mathcal{O}]^b A T^m \exp(-E_a/\mathcal{R}T) \,, \tag{10.97}$$

where the coefficients a, b, A, m, E_a are obtained by fitting experimental data such as flame speed or shock tube induction time. Values derived from flame speed measurements for a variety of fuel-oxidizer systems are given in Westbrook and Dryer (1981). Although this form of the reaction rate is superficially similar to that of elementary molecular reaction rates, the parameters cannot be interpreted in terms of molecular processes and in particular, a and b are not the same as or even related to the stoichiometric coefficients in global reaction R26. The conservation of mass places the following constraint on the reaction rates of each species.

$$0 = \sum_{k=1}^{K} W_k \dot{\omega}_k \,. \tag{10.98}$$

For R26, this becomes

$$0 = W_o \dot{\omega}_{\mathcal{O}} + W_f \dot{\omega}_{\mathcal{F}} + W_p \dot{\omega}_{\mathcal{P}} \,. \tag{10.99}$$

A further constraint is the conservation of each atomic species making up the reactants and products. The reaction R26 must be balanced which constrains the net rates of destruction of the reactants and the production of the products (the reaction is assumed to be irreversible). From the previous discussion on reaction detailed balancing (10.33), we obtain the additional constraint

$$\frac{1}{n_p}\frac{\mathrm{d}[\mathcal{P}]}{\mathrm{d}t} = -\frac{1}{n_o}\frac{\mathrm{d}[\mathcal{O}]}{\mathrm{d}t} = -\frac{1}{n_f}\frac{\mathrm{d}[\mathcal{F}]}{\mathrm{d}t} \,, \tag{10.100}$$

which can be used to define all reaction rates in terms of a single rate of progress $\dot{q}$

$$\frac{1}{n_p}\dot{\omega}_{\mathcal{P}} = -\frac{1}{n_o}\dot{\omega}_{\mathcal{O}} = -\frac{1}{n_f}\dot{\omega}_{\mathcal{F}} = \dot{q} \,. \tag{10.101}$$

One limitation of this approach is that the molar mass and stoichiometric coefficients are constants, so that the composition of the products is fixed. This means that only fixed proportions of the major species can be considered in the products and the dissociation of the products to form minor species is not allowed; the thermodynamics of the products can only be represented very approximately by these models. For example, the stoichiometric reaction of pentane and air would be described by the following global reaction

$$C_5H_{12} + 8O_2 + 30.08N_2 \rightarrow 5CO_2 + 6H_2O + 30.08N_2 \tag{R27}$$

while at typical combustion product temperatures, the major products will actually be a mix of CO, CO_2, H_2O, and H_2 and smaller but still significant amounts of species H, O, and OH will be present. An example of the distribution of the actual equilibrium product species for R27 at 1 atm as a function of temperature is shown in Fig. 10.7.

In terms of the one-step formalism, the products are just the mixture of the CO_2 and H_2. Referring to Fig. 10.7, this is a reasonable approximation for constant-pressure combustion which has an equilibrium product temperature of 2276 K. At higher temperatures that occur for constant-volume ($T = 2650$, $P = 0.96$ MPa) or Chapman-Jouguet detonation equilibrium states ($T = 2847$ K, $P = 1.9$ MPa), minor species are much more important and the major species approximation with only two major product species is increasingly inaccurate. The effect of increased temperature is partially mitigated by the dependence of equilibrium temperature on increased pressure as discussed below.

The nitrogen in the air in considered as a nonreactive diluent that has to be accounted for in computing heat capacity and mass fractions of fuel, oxidizer and products. For a reactive system without diffusive transport of species, the conservation of mass for each species can be written in terms of the single rate of

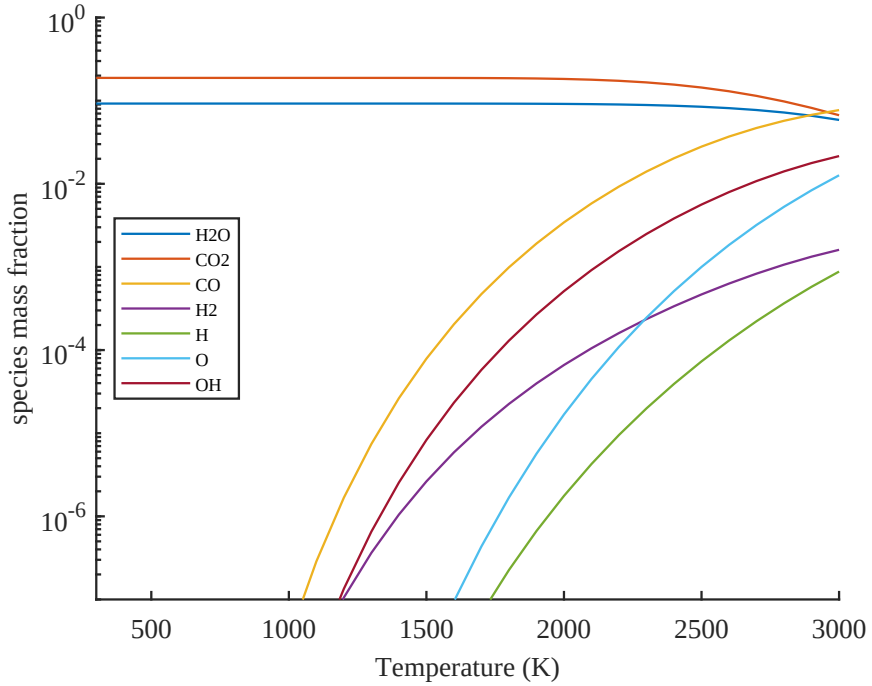

Figure 10.7: Equilibrium product species distribution for R27 as a function of temperature at a pressure of 1 atm.

progress $\dot{q}$:

$$\frac{\mathrm{D}Y_f}{\mathrm{D}t} = -\frac{n_f W_f}{\rho}\dot{q}\,; \tag{10.102}$$

$$\frac{\mathrm{D}Y_o}{\mathrm{D}t} = -\frac{n_o W_o}{\rho}\dot{q}\,; \tag{10.103}$$

$$\frac{\mathrm{D}Y_p}{\mathrm{D}t} = +\frac{n_p W_p}{\rho}\dot{q}\,; \tag{10.104}$$

$$\frac{\mathrm{D}Y_m}{\mathrm{D}t} = 0\,. \tag{10.105}$$

The species $\mathcal{M}$ and the associated mass fraction Y_m represent any nonreactive species like N_2. Consider an initial value situation where we start with known values of fuel and oxidizer which react over time to form products which are initially not present. We integrate the species equations to obtain the following constraints for the mass fractions

$$Y_f(0) = Y_f + \frac{M_f}{M_p}Y_p\,, \tag{10.106}$$

$$Y_o(0) = Y_o + \frac{M_o}{M_p}Y_p\,, \tag{10.107}$$

$$Y_m = Y_m(0)\,, \tag{10.108}$$

where $M_k = n_k W_k$. The conservation of species $\sum Y_k = 1$ provides an additional constraint

$$1 - Y_m = Y_f + Y_o + Y_p = \text{constant} \tag{10.109}$$

To proceed further, we consider an irreversible reaction which results in the complete consumption of reactants as $t \to \infty$

$$Y_f(\infty) = 0\,, \tag{10.110}$$
$$Y_o(\infty) = 0\,, \tag{10.111}$$
$$Y_p(\infty) = 1 - Y_m\,. \tag{10.112}$$

The mass fractions of fuel and oxidizer can now be expressed in terms of the mass fractions of the product and nonreactive species

$$Y_f = \frac{M_p}{M_f}\left(Y_p(\infty) - Y_p\right)\,, \tag{10.113}$$
$$Y_f = (1 - Y_m)\frac{M_p}{M_f}\left(1 - \lambda\right)\,, \tag{10.114}$$
$$Y_o = (1 - Y_m)\frac{M_p}{M_o}\left(1 - \lambda\right)\,, \tag{10.115}$$
$$\lambda = Y_p/Y_p(\infty)\,. \tag{10.116}$$

The variable $0 < \lambda < 1$ is the reaction coordinate or progress variable describing the extent of reaction; $\lambda = 0$ is all reactants, $\lambda = 1$ is all products. The composition and empricial reaction rate expression can be completely specified in terms of λ and the initial state of the mixture using the concentration-mixture fraction relationships

$$[\mathcal{O}] = \rho\frac{Y_o}{W_o}\,, \tag{10.117}$$
$$[\mathcal{F}] = \rho\frac{Y_f}{W_f}\,. \tag{10.118}$$

Substituting into (10.97), we obtain the final equation for the rate of progress of the model one-step reaction

$$\frac{\mathrm{D}\lambda}{\mathrm{D}t} = (1 - Y_m)^{a+b-1}\left(\frac{M_p}{M_f}\right)^a\left(\frac{M_p}{M_o}\right)^b\rho^{a+b-1}(1-\lambda)^{a+b}AT^m\exp(-E_a/\mathcal{R}T)\,. \tag{10.119}$$

The quantity $a + b$ is referred as the *reaction order*. True bi-molecular reactions are second order and unimolecular reactions are first order; the reaction orders for empirical rates of the form (10.97) have orders of approximately 1.75 for most hydrocarbon fuels in air when the metric is flame speed and flammability limit. Typical activation energies are on the order of 30 kcal·mol^{-1}.

Approximate treatments of reaction, particulary in detonation modeling (Fickett and Davis, 1979, Lee, 2008) often simplify the one-step reaction model rate expression to be

$$\frac{\mathrm{D}\lambda}{\mathrm{D}t} = k(1-\lambda)^n\exp(-E_a/\mathcal{R}T)\,. \tag{10.120}$$

Values of $n = 1$ are common although high-explosives researchers often choose $n = 1/2$ and use a pressure rather than temperature-dependent expression.

The thermodynamics of the product state must be approximated in order to use a one-step model in conjunction with either steady or unsteady simulations of fluid motion. The product state is a function of the composition, temperature and pressure. For a fixed pressure, we can evaluate the product state for an equilibrium composition as a function of temperature. The equilibrium product and frozen reactant enthalpy for R27 are shown at three representative pressures in Fig. 10.8. The dissociation of the major species shown in Fig.10.7 results in the nonlinear dependence of product enthalpy on temperatures at sufficiently high temperatures. As discussed previously, the dependence of equilibrium composition on pressure shifts the onset of significant nonlinearity to higher temperatures at higher pressures. The approximate linearity of the enthalpy-temperature relation at sufficiently low temperatures is the motivation of the approximate models discussed next.

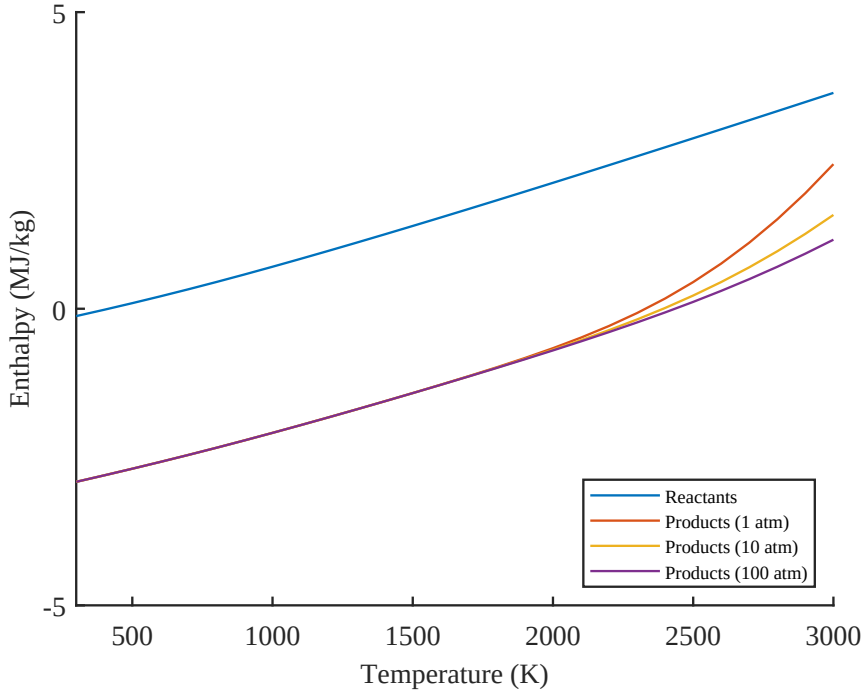

Figure 10.8: Equilibrium product enthalpy for R27 as a function of temperature at pressures of 1, 10 and 100 atm.

The simplest sort of thermodynamic model is a constant-γ, constant molar-mass, fixed-energy release function for the specific internal energy

$$e = \frac{P/\rho}{\gamma - 1} - \lambda q \,, \tag{10.121}$$

or equivalently, enthalpy

$$h = \frac{\gamma P/\rho}{\gamma - 1} - \lambda q \,. \tag{10.122}$$

Values of γ and q are selected to mimic the properties of a particular chemical system. A slightly more realistic model is to assume that the specific heats for reactants and products take on different values as in the two-γ model described in Section A.5. The mixture specific enthalpy can be approximated as

$$h = (1 - Y_m)\left[(1-\lambda)h_r(T) + \lambda h_p(T)\right] + Y_m h_m(T) \,, \tag{10.123}$$

for fixed composition in each constituent. This can be reorganized to separate the contributions of the reaction to the change in enthalpy

$$h = (1-\lambda)\left[(1 - Y_m)h_r(T) + Y_m h_m(T)\right] + \lambda\left[Y_m h_m(T) + (1 - Y_m)h_p(T)\right] \,. \tag{10.124}$$

In the notation of Section A.5, the correspondence to the one-step enthalpies is

$$h_1(T) = Y_m h_m(T) + (1 - Y_m)h_r(T) \,, \tag{10.125}$$

and

$$h_2(T) = Y_m h_m(T) + (1 - Y_m)h_p(T) \,. \tag{10.126}$$

The final reduction to the two-γ model form requires further simplification by taking the specific heat to be a constant for each constituent group and approximating the enthalpy as

$$h \approx c_p T + h_0 \,. \tag{10.127}$$

The energy release parameter is

$$q = h_{0,1} - h_{0,2} \,, \tag{10.128}$$

or in terms of the actual reactant and product properties

$$q = (1 - Y_m)\left[h_r(0) - h_p(0)\right] \,. \tag{10.129}$$

The values of the specific heat c_p and constant h_0 for the two-γ model approximation have to be determined by fitting the actual thermodynamic data over the range of (T, P) of interest. The effective values of the specific heat ratios are:

$$\gamma_1 = \frac{c_{p,1}}{c_{p,1} - R_1} \,, \qquad \gamma_2 = \frac{c_{p,2}}{c_{p,2} - R_2} \,. \tag{10.130}$$

For the example of R27, the linear model (10.127) for reactant and product enthalpy can be implemented by using the least-squares method to obtain the slope and intercept of lines fit to evaluation of mixture enthalpy. The fit is limited to temperature values less than the maximum that results in significant departure from linearity. For the a pressure of 1 atm, this is a temperature of approximately 2300 K. The resulting fits obtained by demo_eq_one_step.m are shown in Fig. 10.9. The values for the thermodynamic coefficients

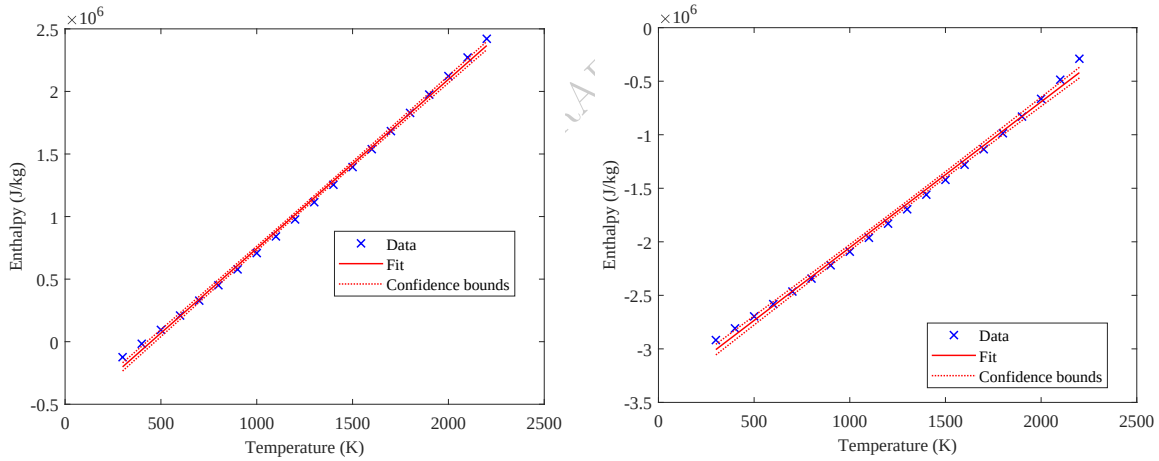

Figure 10.9: Linear fits to reactant (a) and equilibrium product (b) enthalpy for R27 as a function of temperature at a pressure of 1 atm.

obtains from the fits in Fig. 10.9 are given in Table 10.1 as the "low-temperature" set of parameters. An alternative procedure is to use the CJ state to create a thermodynamic model as described in Section 6.7 and A.3. These values of the product specific heat, γ and the value of enthalpy intercept h_0 for CJ state products are substantially different than the low temperature fit values due to higher temperature resulting in more dissociation in the products and also the choice of equilibrium values rather than frozen for the specific heat with corresponding value of γ). The product specific heat was obtained by fitting the product isentrope originating at the CJ state, which approximates typical expanded states encountered in compressible flow simulations of detonation wave dynamics. Fig. 10.9.

The value of h_{02} was computed using the effective value of $q =$ that matches $M_{\rm CJ} = 5.3814$ and the value of h_{01} determined from the reactant fit at low temperature. The program demo_CJstate_isentrope.m was

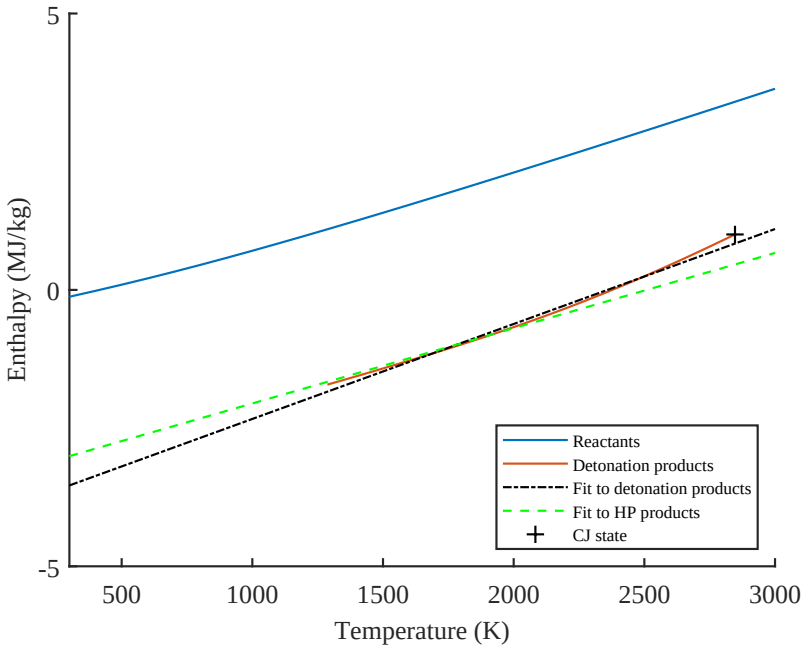

Figure 10.10: Comparison of stoichiometric pentane-air $h(T)$ for reactants and products (CJ isentrope) as well as low and high-temperature linear fits to equilibrium product enthalpy.

used together with a minimal set of major and minor species (nC_5H_{12}, N_2, O_2, H_2O, CO_2, CO, H_2, H, O, OH) in pentane_thermo.cti in order to reduce computation time yet still get accurate results for the equilibrium products. A comparison between the reactant and product $h(T)$ relationships for realistic thermodynamics as well as the low and high-temperature linear fits was computed with demo_eq_one_step.m and is shown in Fig. 10.10.

Table 10.1: Themodynamic parameters for one-step model of R27.

	c_p (J·kg^{-1}·K^{-1})	h_0 (J·kg^{-1})	W (kg·kmol^{-1})	γ
Low-temperature, $T < 2300$ K.				
reactants	1351.5	-6.069×10^5	29.96	1.2584
products	1361.3	-3.415×10^6	28.50	1.2727
High-temperature, CJ isentrope				
products	1718.0	-4.035×10^6	27.83	1.2105

Using the NASA-7 format of the thermodynamic data for the Cantera `.cti` file as described in Section 5.1, the linear fit coefficients will be of the form

$$\begin{aligned}\text{thermo} = (&\,\text{NASA}([200,\ 1000],\ [c_p/R,\ 0,\ 0,\ 0,\ 0,\ h_0/R,\ s_0/R]),\\ &\,\text{NASA}([1000,\ 6000],\ [c_p/R,\ 0,\ 0,\ 0,\ 0,\ h_0/R,\ s_0/R])\,)\ .\end{aligned}$$

Because we are using a constant and equal specific heat for both the first and second segment of the fit, the values for the minimum, midpoint and maximum temperature are arbitrary so we have used nominal values. Unless we are considering a specific family of solutions with reversibility between reactants and

products (Kao, 2008), the values of s_0/R can be chosen to be zero for reactants and sufficiently large (s_0/R = 10) for the products to create an effectively irreversible reaction. A drawback to this approach is that the molar mass of reactants and products must be equal because Cantera requires conservation of elements and mass in the reactions and in the equilibrium algorithm.

Two `.cti` files with the thermodynamic model and several one-step reaction models are provided in pentane_two_gamma.cti (low-temperature fit) and pentane_two_gamma_CJ.cti. The effect of choice of reaction order using the two-γ, one-step model is shown in Fig. 10.11. The values of A have been adjusted for each order so that the induction time based on the maximum temperature time derivative is 5.5×10^{-6} s, the same as predicted by the detailed reaction mechanism simulation.

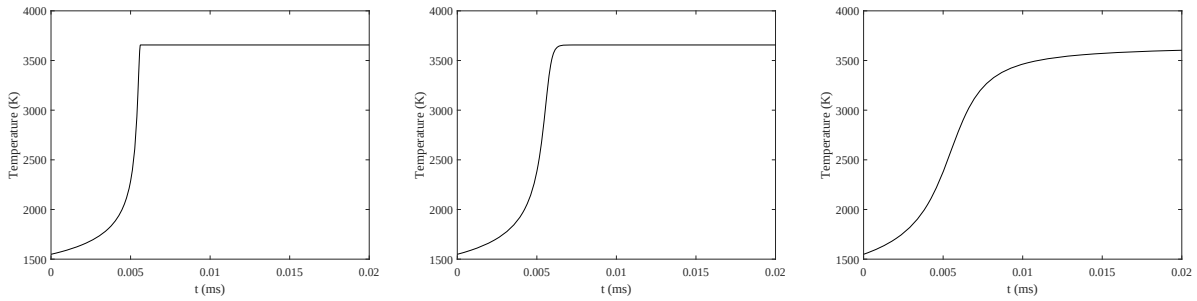

(a) (b) (c)

Figure 10.11: Example constant-pressure combustion simulation with two-γ, one-step reaction model $k = A(1-\lambda)^n \exp(-E/\mathcal{R}T)$, $E_a = 30$ kcal $\cdot$ mol^{-1}. a) $n = 1/2$, $A = 5.15\times10^6$. b) $n = 1$, $A = 3.6\times10^8$. c) $n = 2$, $A = 1.7\times10^{12}$. The initial conditions are $P_0 = 3.49$ MPa; $T_0 = 1549$ K, the vN state for a stoichiometric pentane-air CJ detonation .

We can create a slightly better one-step model for Cantera with more realistic thermodynamics and different molar masses for reactants and products by using a mixture of the actual reactant species and major products. This will properly simulate the change in the number of moles or equivalently average molar mass between reactants and products as well as the dependence of the enthalpy of those species on temperature. This will also enable the use of empirical reaction rate expressions of the form (10.97). The pentane_one_step.cti file takes this approach.

In the `.cti` file, the empirical reaction is balanced as in R27 but empirical reaction orders are specified as shown in (10.97) instead of using the stoichiometric coefficients from the balanced reaction. However, the thermodynamic state of the products will still not be quite correct as the effect of dissociation is not taken into account because only N_2,CO_2 and H_2O are used as product species. A polynomial curve could be fit to the equilibrium enthalpy to take account of the nonlinearity in enthalpy vs temperature, however the change in molar mass of the products will not be accounted for unless those species and the associated reactions are included. If more realistic results are needed for equilibrium or chemical reaction rate computations, a realistic set of species has to be used.

One-step reactions may be directly specified as an overall reaction rate k of the form (10.97), e.g, Westbrook and Dryer (1981) and the reaction progress computed from

$$\frac{\mathrm{d}[\mathcal{F}]}{\mathrm{d}t} = \dot{\omega}_{\mathcal{F}} \,, \tag{10.131}$$

$$\frac{\mathrm{d}[\mathcal{F}]}{\mathrm{d}t} = -k \,. \tag{10.132}$$

For example, Westbrook and Dryer gives the following reaction rate as being appropriate for low-pressure flame simulations for pentane-air combustion

$$k = 6.4 \times 10^{11} \exp(-30000/\mathcal{R}T)[\mathrm{nC_5H_{12}}]^{0.25}[\mathrm{O_2}]^{1.5} \tag{10.133}$$